SUPPLEMENTARY DATA

Figure 1 Phenotyping of *LFA-1*$^{+/+}$ and *LFA-1*$^{-/-}$ CD4 T cell populations before and after adoptive transfer into WT host mice. (A) FACS analysis of the initial populations of *LFA-1*$^{+/+}$ and *LFA-1*$^{-/-}$ CD4 T cells highlighting comparable proportions of the major subset of naïve cells (CD62L+, CD44^{lo}); typical data for n=6 mice/group. **(B)** Adoptively transferred *LFA-1*$^{+/+}$ and *LFA-1*$^{-/-}$ CD4 (CD62L+, CD44^{lo}) T cells (5x10^6 per cell type) in LN of WT host mice at 6 h; the CD44 versus CD62L analysis was gated on CFSE$^+$ (*LFA-1*$^{+/+}$*)* and SNARF-1$^+$ (*LFA-1*$^{-/-}$*)* cells; experiment contemporaneous with (**A**); typical data for n=6 mice/group. **(C)** Blocking effect on T cell entry into LN following treatment with L-selectin/α4 mAbs. To ensure that further entry of both *LFA-1*$^{+/+}$ and *LFA-1*$^{-/-}$ T cells were equally blocked, L-selectin mAb MEL-14 and α4 integrin mAb PS2/3 or PBS as a control were injected 30 min prior to the fluorochrome-labelled T cells (5 x10^6 per cell type), then T cell numbers were assessed 4 h later. Following this treatment, *LFA-1*$^{+/+}$ and *LFA-1*$^{-/-}$ T cell entry were both blocked by >99% (see text). To ensure the efficiency of the mAb blocking regime, the protocol was carried out contemporaneously with the LN trafficking experiments.

Figure 2. Phenotypic details of lymphatic vessels in the inguinal LN.

(A) Tiled image of pLN showing distribution of LYVE-1-expressing LV. Additionally illustrated are subcapsular sinus, T zone and medulla for orientation; inset area showing fine detail of the LV sinuses extending from the (para-)cortical T zone (upper left corner of inset) to the subcapsular sinus (lower right corner of inset). Alexa 546- or Pacific Blue-conjugated LYVE-1

mAb was injected into the flank of a mouse near the inguinal LN and labeling of LV observed after 16-24 hr. **(B)** Tiled image of pLN showing distribution of s.c applied FITC-dextran (2 MDa)(green) to illustrate overlap with LYVE-1^+ LV (blue); inset areas show detail of the cortical (inset 1) and medullary (inset 2) sinuses. Flow of lymphatic fluid is confirmed by the spread of 2 MDa FITC-dextran (green) throughout the network with pattern generally overlapping Pacific blue-conjugated LYVE-1 labeling (blue). The FITC-dextran was concentrated in the subcapsular sinus region, but extended into the lymphatic vessels in the cortical region (**inset 1**) and into the medulla (**inset 2**)**.**

Figure 3. Transwell assay showing migration of primary LFA-$1^{+/+}$ and LFA-$1^{-/-}$ CD4 T cells on ICAM-1-coated filters. The fold induction of T cell migration over 1.5 h in response to 25 nM S1P and 6 μM CCL21 in the lower chamber is shown; filters were coated with mouse ICAM-1Fc at 1 μg/ml overnight and T cells were pre-incubated in fatty acid free BSA for 4 h prior to the experiment; data averaged from n=4 experiments.

Figure 4. Intranodal T cell motility and peripheral lymphopenia upon administration of FTY720. (A) Intravital microscopy of T cell velocity in the inguinal lymph node of the mouse (paracortical T zone, 150 μm depth) at 8 hr after administration of FTY720 or PBS; mice were treated with FTY720 (Cayman Chemical Company, Ann Arbor, MI, USA) i.p. at 1 mg/kg, following a regime previously shown to be effective for at least 20 hr (Cinamon *et al* Nat. Immunol. 5, 713-20 2004; Brown *et al*, J. Immunol. 185, 4873-82, 2010); **(B)** Blood cells counts for PBL, B cells, and CD4+ T cells as measured by flow

cytometry. In untreated animals, this resulted in ~20,000 total peripheral blood leucocytes (PBL) events per sample. Data are from two independent experiments with a total of 4 and 5 mice each for intravital analysis of T cell motility and FACS analysis of blood cell counts respectively. For intravital analysis of T cell motility, 100 T cells per experiment were counted.

Figure 5. *LFA-1*$^{+/+}$ and *LFA-1*$^{-/-}$ T cell associations with tubular LVs in the peripheral medullary region of the T zone.

(**A**) Intra-vital microscope image of *LFA-1*$^{-/-}$ and *LFA-1*$^{+/+}$ CD4 cells associated with LYVE-1+ tubular LV area at 50-80 μm depth, intermediate between paracortical T zone and medulla; macrophages (auto-fluorescent, white) are associated with the LV in this region; scale bar=50 μm. **(B)** Quantification data for T cell velocity in areas with x-y axes of 250 μm; data combined from 3 experiments with >50 cells analysed per T cell type.

Figure 6. Expression of the LFA-1 ligand ICAM-1 on LYVE-1-positive lymphatic vessels and MOMA-1/CD169-positive macrophages in the medulla area. Sections of inguinal lymph node (see Fig. 8a) were stained for ICAM-1 (red), LYVE-1 (green) and MOMA-1/CD169 (blue) and co-expression (merge) was viewed by confocal microscopy (63x, LSM 710); scale bar=30 μm.

Figure 7. Lack of effect of swapping the fluorescent dyes used for intravital staining of T cells (to accompany Fig. 6). There were no effects of colour swap on **(A)** velocity of *LFA-1*$^{-/-}$ and *LFA-1*$^{+/+}$ T cells or **(B)** their

observed morphological differences when viewed by intravital microscopy. The T cells displayed equivalent differences when labelled with SNARF (red) or CFSE (green) when migrating in the branched LV network of the medulla.

Video 1. Demonstration of T cell velocity in different zones of the LN. The movie shows the high motility of T cells within the T zone (left) and slow to arrested motion of the cells at the rim of the T zone in the highly branched LV network of the medulla region (right). *LFA*$^{+/+}$ T cells (green, quenched in the blue zone); *LFA-1*$^{-/-}$ T cells (red); LYVE-1^{+} LV (blue); auto-fluorescent macrophages (white); section width is 300 µm; projection view of a 7 x 5 µm z-stack; images taken every 30 sec; duration: 20 min.

Video 2. Flow in an efferent lymphatic vessel leading from an inguinal lymph node. Monitoring of flow in an efferent vessel of inguinal lymph node following injection of FITC-Dextran (2 MDa, green) s.c. into the footpad at 2.5 h before imaging. Blue: Vessel walls (SHF, second harmonic generation signal of collagen fibers); interval between frames, 16 sec, duration: 2 h.

Video 3. Motility of T cells contacting a tubular LYVE-1+ LV adjacent to the paracortical T zone. *LFA-1*$^{+/+}$ T cells (green), *LFA*$^{-/-}$ T cells (red) are crossing into and out of the LYVE-1^{+} LV (blue); detail of two LV in cross section outlined in white showing 4 *LFA-1*$^{-/-}$ T cells (circled, red) making contact and entering the vessels and 3 *LFA-1*$^{+/+}$ T cells (circled, green) behaving similarly, but leaving the vessel area following LV probing; section

width is 200 µm; projection view of a 7 x 5 µm z-stack; images taken every 30 sec; duration: 30 min.

Video 4. Detail of the behaviour of *LFA-1*$^{+/+}$ and *LFA-1*$^{-/-}$ T cells migrating on LYVE-1 lymphatic vessel network in the region of the medulla. *LFA-1*$^{+/+}$ T cells (green) arrest more frequently and remain visible, while *LFA-1*$^{-/-}$ T cells (red) show straighter paths of movement and disappear into the LYVE-1+ lymphatic meshwork (blue) over time. The section width is 300 µm; images taken every 4 sec; duration: 9.3 min.

Supplementary Figure 1

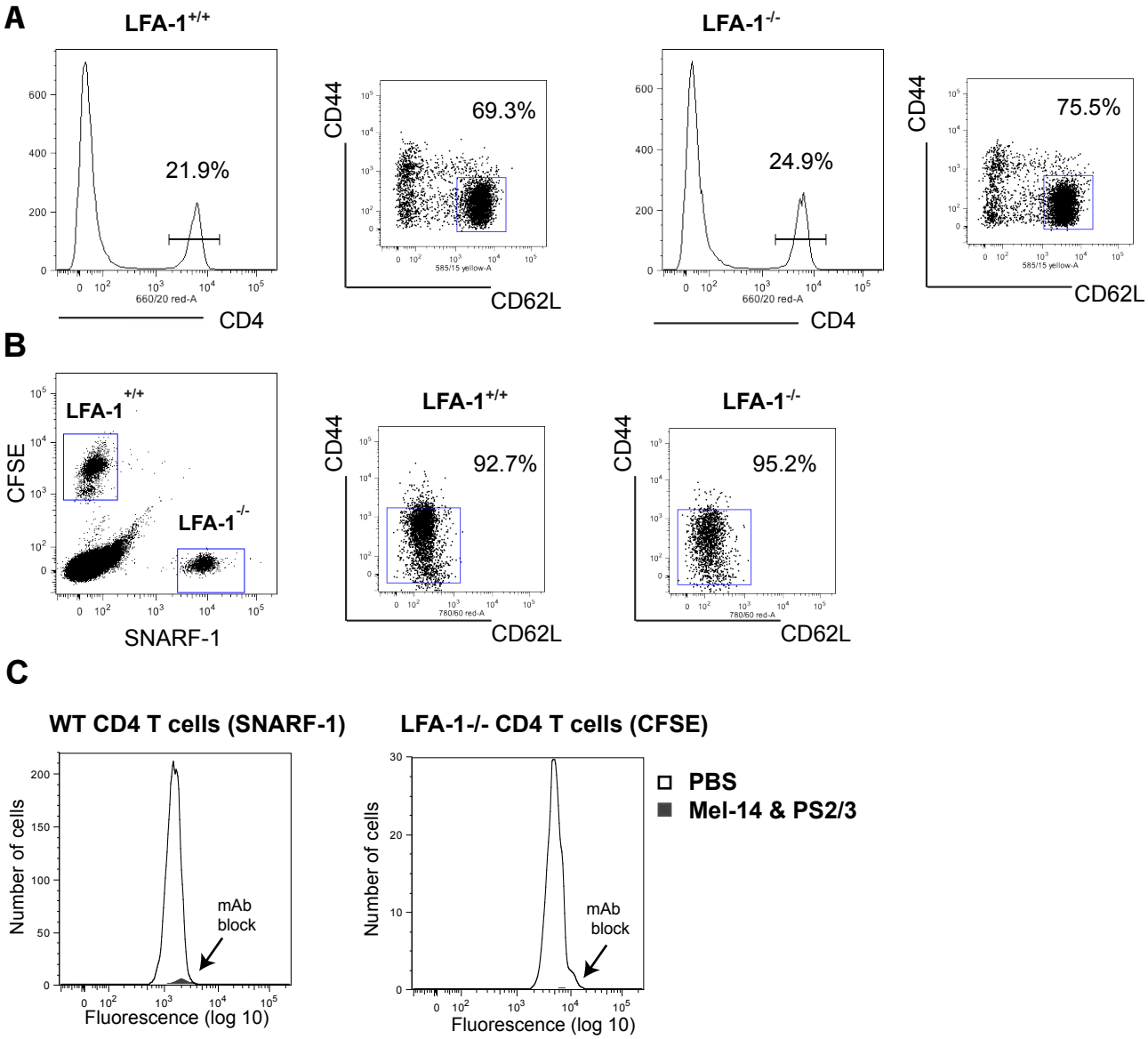

Supplementary Figure 2

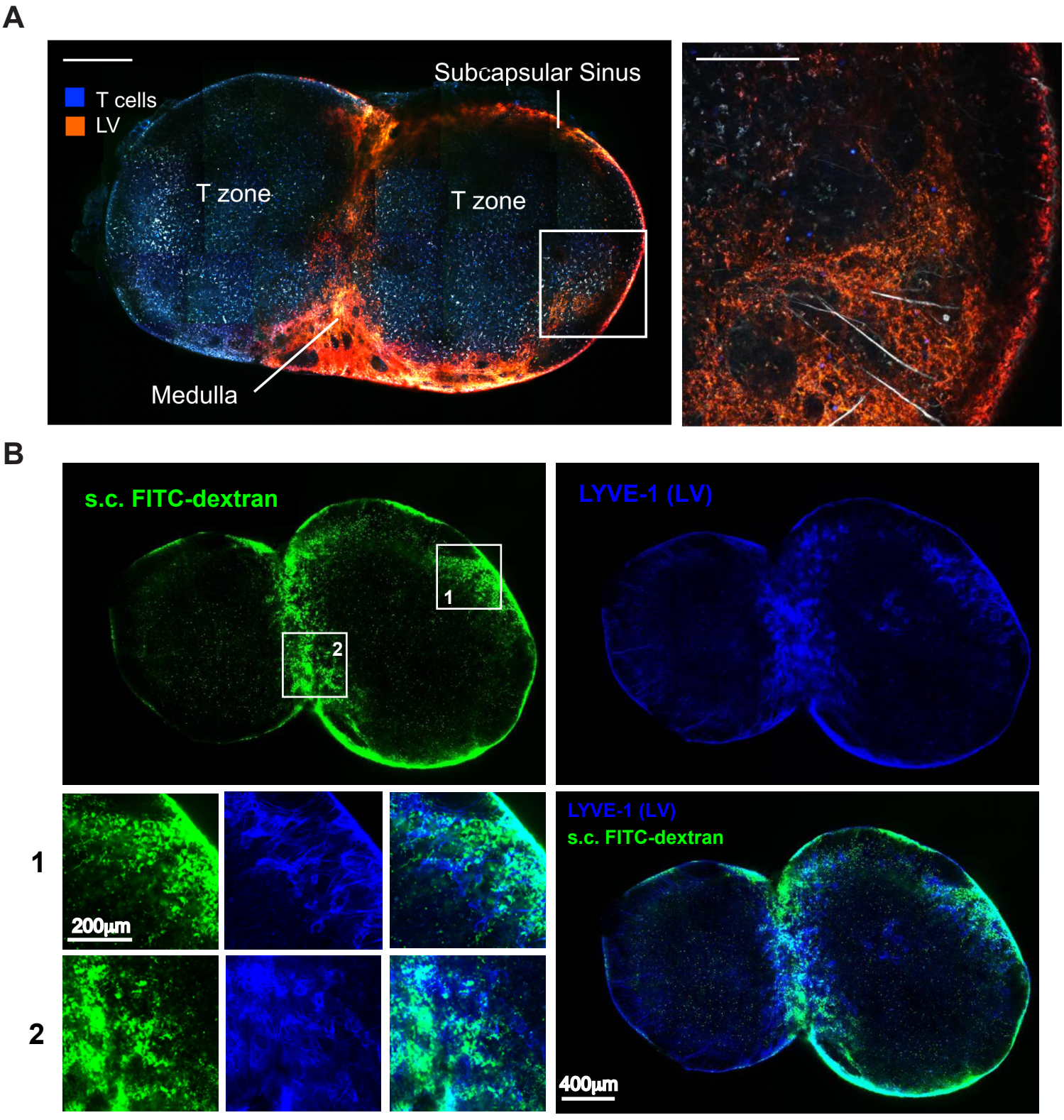

Supplementary Figure 3

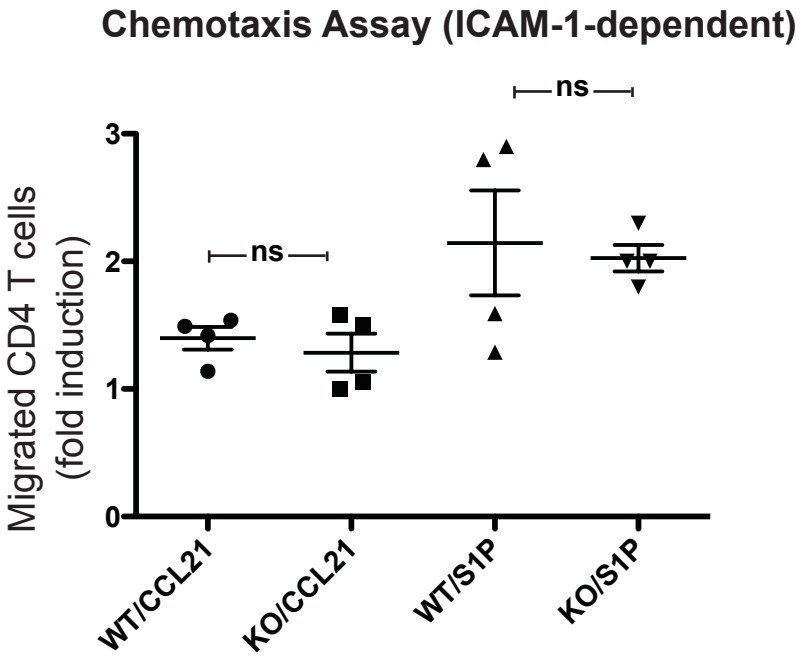

Supplementary Figure 4

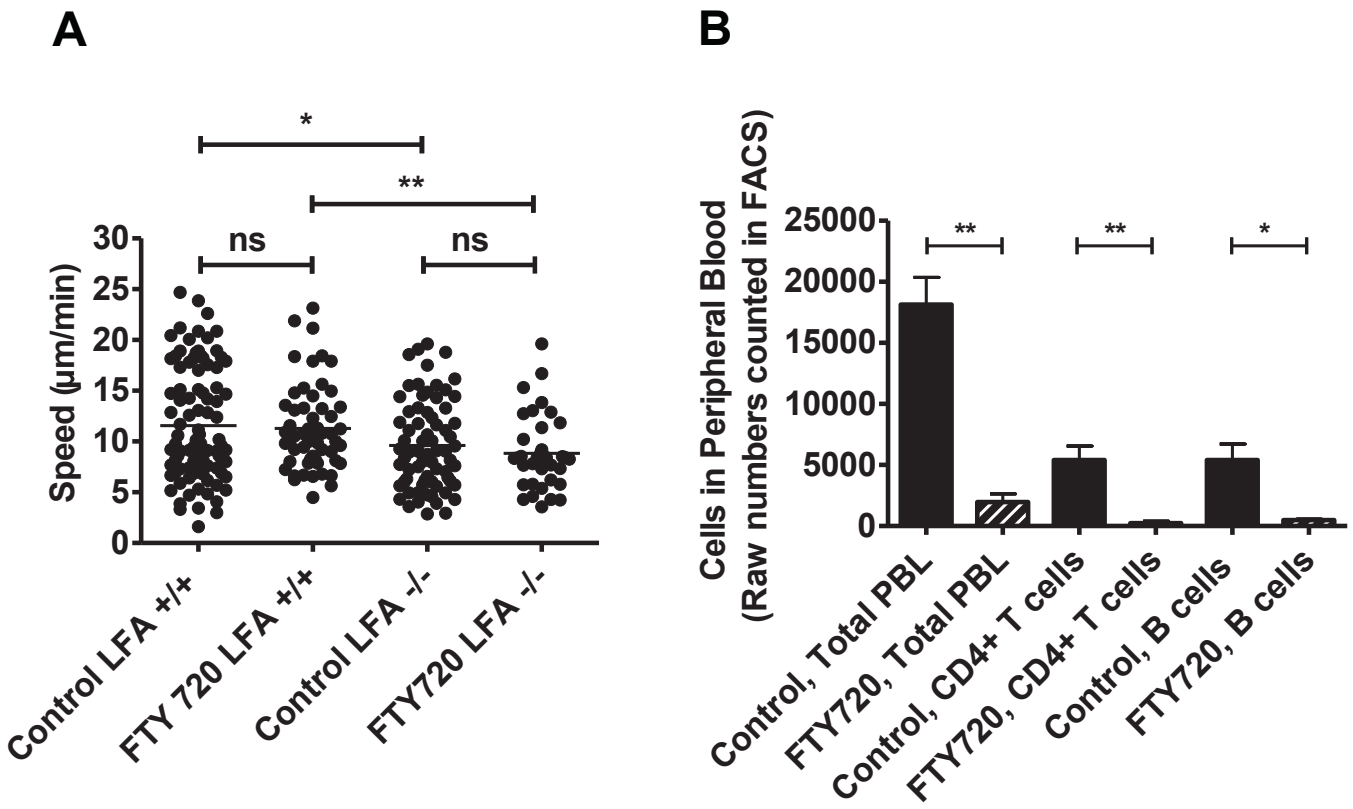

Supplementary Figure 5

A

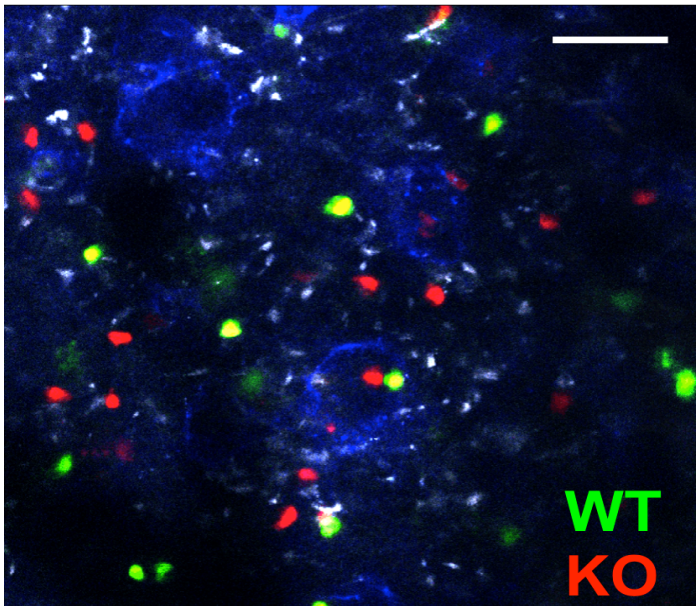

B

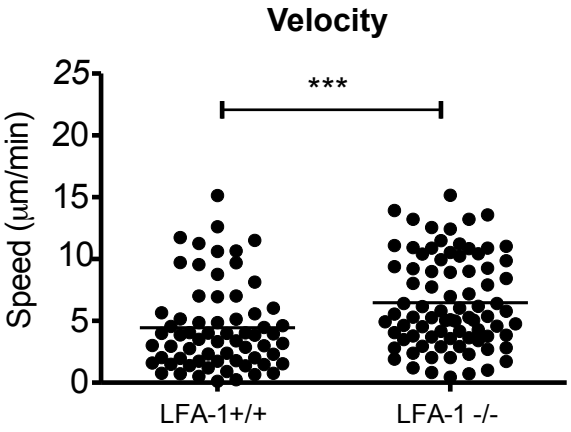

Supplementary Figure 6

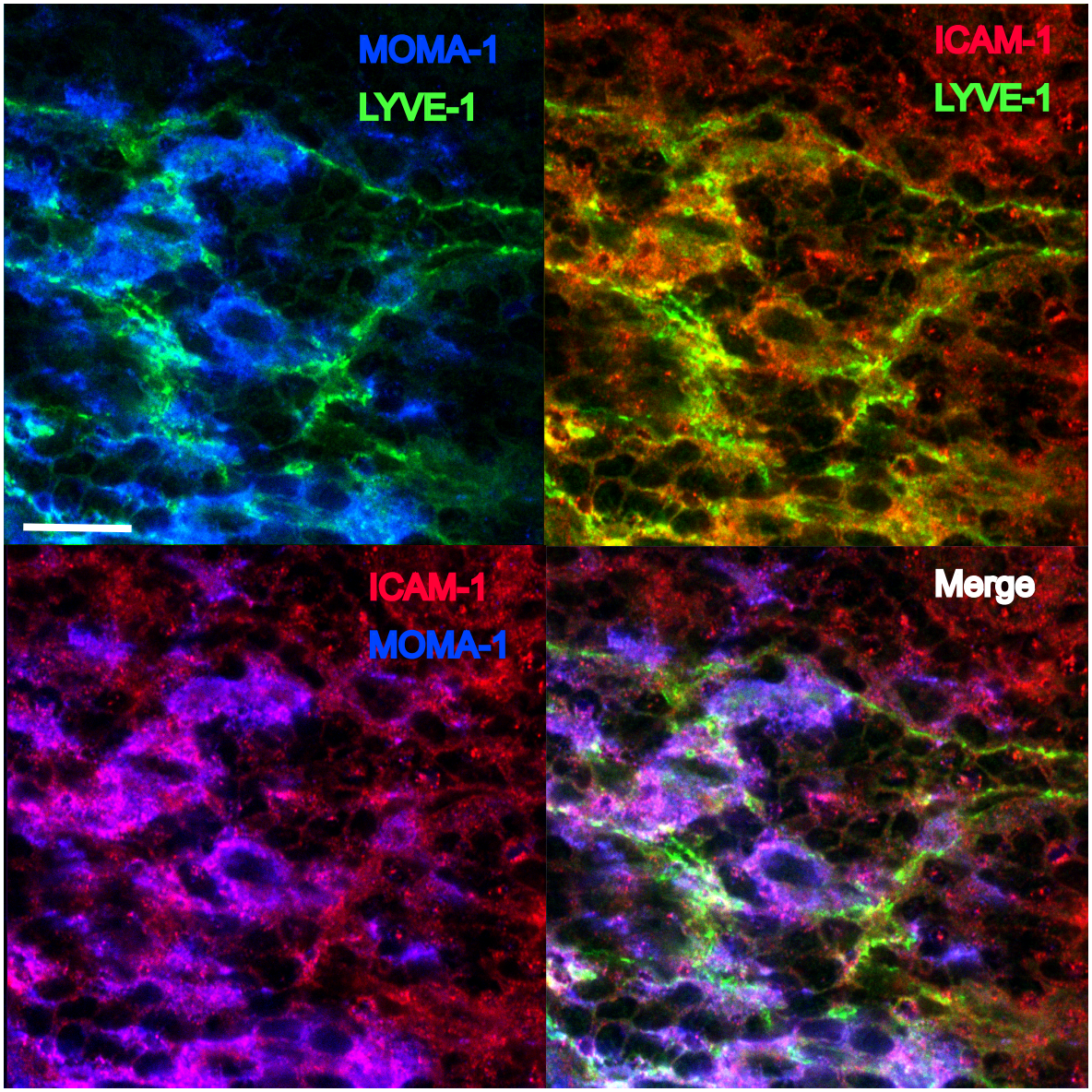

Supplementary Figure 7

A Velocity at distal LV (Fig. 6C)

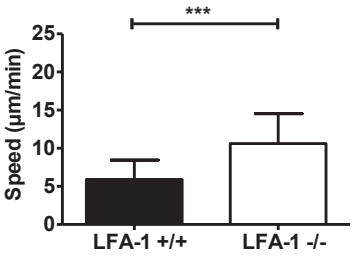

LFA-1+/+ cells stained CFSE (green)

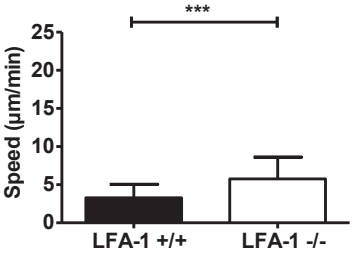

LFA-1+/+ cells stained SNARF (red)

B Axis ratio (Fig. 6D)

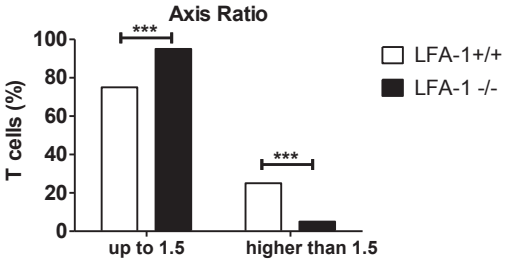

LFA-1+/+ cells stained CFSE (green)

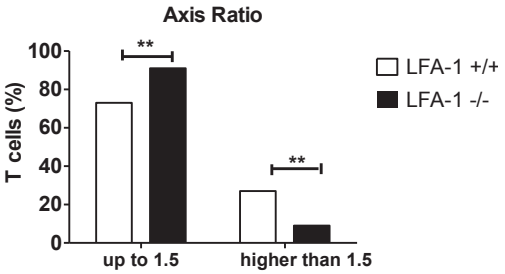

LFA-1+/+ cells stained SNARF (red)